STRUCTURE AND IDENTIFICATION OF TRANSIENT AND EQUILIBRIUM PHASES IN Mg ALLOYS CONTAINING RARE-EARTH ELEMENTS

BOHUMIL SMOLA[1,2]*, IVANA STULÍKOVÁ[1,2]

An overview of structure and morphology of transient and equilibrium phases in magnesium alloys with rare-earth elements is given here. Problems and peculiarities of the phase structure determination, phase identification and recognition by transmission electron microscopy and electron diffraction are discussed.

K e y w o r d s: magnesium alloys, rare-earth, electron diffraction, transmission electron microscopy, precipitation, decomposition sequence

STRUKTURA A IDENTIFIKACE NEROVNOVÁŽNÝCH A ROVNOVÁŽNÝCH FÁZÍ VE SLITINÁCH Mg OBSAHUJÍCÍCH PRVKY VZÁCNÝCH ZEMIN

Je podán přehled struktury a morfologie nerovnovážných a rovnovážných fází vyskytujících se ve slitinách hořčíku se vzácnými zeminami. Jsou diskutovány problémy a zvláštnosti, které mohou nastat při určení struktury fází, identifikaci a rozlišení fází pomocí transmisní elektronové mikroskopie a difrakce elektronů.

1. Introduction

Alloying magnesium with rare-earth elements (R.E.), inclusive Y, is used to develop light construction alloys for the applications at elevated and high temperatures, e.g. [1–4]. The knowledge of the precipitation microstructure (phase structure, morphology, volume fraction, density, shape and size, orientation relationship to the matrix etc.) responsible for the alloy properties is there of primary importance. Mainly transient phases precipitating during decomposition of super-saturated solid solution produce the peak mechanical properties (hardness, yield

[1] Faculty of Mathematics and Physics, Charles University, Ke Karlovu 5, Prague 2, Czech Republic
[2] Zentrum für Funktionswerkstoffe gGmbH, Sachsenweg 8, Clausthal-Zellerfeld, Germany
* corresponding author, e-mail: bohumil.smola@mff.cuni.cz

and ultimate tensile stress, creep resistance) [3, 5–7] if dense dispersed and rationally oriented in the matrix [8], similarly as rationally oriented plate- or rod-shaped precipitates in Al alloys [9]. The structure determination of phases present in Mg-R.E. base alloys after a heat treatment may be complicated. The volume fraction and/or size of the phases precipitated is usually low, their plane spacings are similar and the occurrence temperature ranges overlap. Two basic sequences of the decomposition of supersaturated solid solution are known in binary Mg-R.E. alloys, namely:

Mg-Gd (Y) type [1, 5, 10]: $\alpha'(\text{cph}) \rightarrow \beta''$ (D0_{19}) $\rightarrow \beta'(\text{Cbco}) \rightarrow \beta(\text{fcc, bcc})$,

Mg-Ce type [1, 5]: $\alpha'(\text{cph}) \rightarrow \beta''(\text{D0}_{19}) \rightarrow \beta'(\text{fcc}) \rightarrow \beta(\text{bct})$.

The β'' transient phase has hexagonal D0_{19} structure ($a = 2 \cdot a_{\text{Mg}}$, $c = c_{\text{Mg}}$) and is coherent to the close packed hexagonal α'-Mg matrix in both decomposition sequences. The β'(Cbco – C base-centred orthorhombic, $a = 2 \cdot a_{\text{Mg}}$, $b \cong 8 \cdot d(1\bar{1}00)_{\text{Mg}}$, $c = c_{\text{Mg}}$) is transient phase semicoherent to the α'-Mg matrix in Mg-Gd type sequence. The equilibrium β phase in this sequence is either face centred cubic (Mg_5Gd, $a \cong 8 \cdot d(1\bar{1}00)_{\text{Mg}}$) or body centred cubic (Mg_{24}Y_5, $a \cong 4 \cdot d(1\bar{1}00)_{\text{Mg}}$). The β' transient phase following D0_{19} phase in the Mg-Ce type sequence has fcc structure (D0_3, $a = 0.74$ nm, $\text{d}(220) \cong \text{d}(0002)_{\text{Mg}}$). The equilibrium β phase of this sequence has body centred tetragonal structure (Mg_{12}Ce, $\text{Mg}_{41}\text{Nd}_5$).

These decomposition sequences can be modified in Mg alloys with combination of R.E. from different groups (Gd and Ce) and in complex alloys with the addition of another elements [11–13]. Modification of precipitation sequences and phase morphology may depend not only on the alloy composition but also on casting technology and thermomechanical treatment. Transmission electron microscopy (TEM) and electron diffraction (ED), preferably supported also by energy dispersive analysis of X-ray (EDAX), are the essential methods for determination of phase composition, structure and morphology, especially in the case of low and very low volume fractions and nano-size of phases involved. The present paper summarises the current knowledge of the structure and morphology of transient and equilibrium phases in Mg-R.E. based alloys and the peculiarities and possible problems encountered in the course of their analysis by TEM and ED.

2. Structure and morphology of phases in Mg alloys with R.E. elements

Most of transient and equilibrium phases of the decomposition sequences of Mg-R.E. alloys precipitate as plates with the habit plane parallel to the first or second order prismatic planes of the α'-Mg matrix ($\{1\bar{1}00\}$ or $\{11\bar{2}0\}$, respectively). GP zones reported to form in the pre-precipitation stage of Mg-Nd decomposition sequence [1, 5] were also plates or rods lying in $\{1\bar{1}00\}$ prismatic planes of the α'-Mg matrix.

Table 1. Overview of the occurrence conditions and orientation of β'' phase ($D0_{19}$)

Alloy composition [wt.%]	Treatment; temperature [°C] not plate-like shape	Habit plane of plates	Ref.
Mg-3 Nd	isothermal; 200–300	$\{1\bar{1}00\}_{Mg}$	[5]
Mg-5.08Y-2.96Nd-0.4Zr	isothermal 175, 200	$\{1\bar{1}00\}_{Mg}$	[5]
Mg-6.85MM-1.82Nd-0.52Zr MM = 75 % Y + 25 % heavy R.E.	isothermal 175, 200	$\{1\bar{1}00\}_{Mg}$	[5]
Mg-9.33Gd, Mg-14.55Gd	isochronal 180, 200 fine spherical	-	[10]
Mg-2.985Nd	isothermal 180-260	$\{11\bar{2}0\}_{Mg}$	[23]
Mg-4Y-2.25Nd-0.6Zr	isothermal 150, 250; plates or rods	$\{1\bar{1}00\}_{Mg}$	[12]
Mg-7Gd-2.25Nd-0.6Zr	isothermal 150; plates or rods	$\{11\bar{2}0\}_{Mg}$	[12]
Mg-7Dy-2.25Nd-0.6Zr	isothermal 150; plates or rods	$\{11\bar{2}0\}_{Mg}$	[12]
Mg-4Y-3.3R.E.-0.5Zr(WE43)	isothermal 150;	$\{11\bar{2}0\}_{Mg}$	[14]
Mg-4Y-3.3R.E.-0.5Zr(WE43)	isothermal 150; monolayer plates	$\{1\bar{1}00\}_{Mg}$	[14]
Mg-4Y-3.3R.E.-0.5Zr(WE43)	isothermal 250;	?	[14]
Mg-9.5Gd-3Nd-0.4Zr Mg-9.3Dy-3.2Nd-0.4Zr Mg-10.8Gd-3Y-0.45Zr Mg-10.8Gd-6.6Y-0.36Zr	isothermal 225, 16–64 h $D0_{19}$coexists with Cbco	? $\{1\bar{1}00\}_{Mg}$	[24]
Mg-3Gd-8Y-0.8Zr Mg-6Gd-5Y-0.8Zr Mg-10Gd-3Y-0.7Zr	isothermal 225, 128 h isothermal 225, 32 h isothermal 225, 8 h $D0_{19}$coexists with Cbco	?	[7]
Mg-16.9Gd-0.51Zr Mg-12Gd-1.9Y-0.69Zr Mg-9.3Gd-4.1Y-0.7Zr	isothermal 250, ∼ 100 h $D0_{19}$coexists with Cbco	?	[25]
Mg-5.5Y-2Nd-2R.E.-0.4Zr(WE54)	250, 1–4 h ($D0_{19}$ structure not proved)	$\{11\bar{2}0\}_{Mg}$	[11, 15, 16]
Mg-1.3Ce	isothermal 200, 35 ks a stepped quasi $D0_{19}$ and $D0_{19}$	$\{1\bar{1}00\}_{Mg}$	[26]
Mg-1.3Nd	isothermal 200, 3.6 ks a stepped quasi $D0_{19}$ and $D0_{19}$	$\{1\bar{1}00\}_{Mg}$ $\{11\bar{2}0\}_{Mg}$	[26]
Mg-1.3MM (50 % Ce, 25 % La, 20 % Nd)	isothermal 150, 360 ks a stepped quasi $D0_{19}$ and $D0_{19}$	$\{11\bar{2}0\}_{Mg}$	[26]

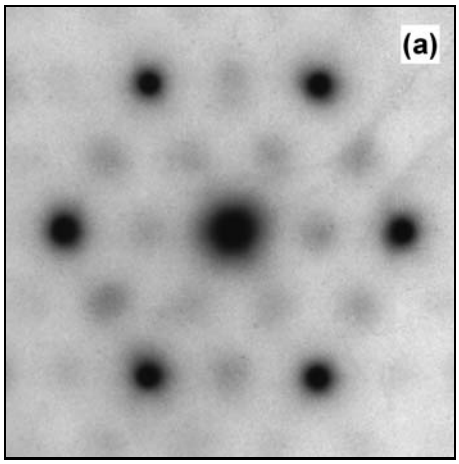

Fig. 1a. ED pattern of Mg15Gd alloy with fine β'' ($D0_{19}$) particles.

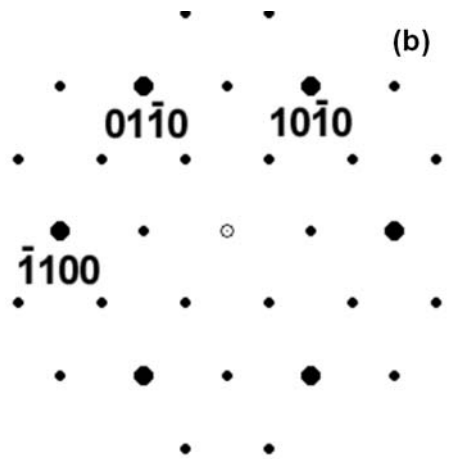

Fig. 1b. Simulated patterns of a), overlapping [0001] patterns of α'-Mg matrix and $D0_{19}$.

2.1 β'' transient phase ($D0_{19}$)

Coherent hexagonal β'' ($D0_{19}$, hP8, $P6_3/mmc$) phase was mostly reported to have $\{1\bar{1}00\}_{Mg}$ as the habit planes, see Table 1. Recent studies done by high resolution TEM (HRTEM) revealed that the β'' plates form also parallel to $\{11\bar{2}0\}_{Mg}$ prismatic planes in some alloys – Table 1 [12, 14]. Platelets parallel to $\{11\bar{2}0\}_{Mg}$ found in commercial alloy WE54 [11, 15] are therefore most probably of the β'' phase.

In the early stages of the α'-Mg matrix decomposition or if the super-saturation is low, the β'' phase particles are very fine and have rather spherical shape. It manifests itself by diffuse diffraction spots in ED patterns, see Fig. 1a [10]. The hexagonal β'' phase has following equiaxial orientation relationship to the cph α'--Mg matrix:

$$\langle 11\bar{2}0\rangle_{\beta''} \| \langle 11\bar{2}0\rangle_{Mg},$$
$$(0001)_{\beta''} \| (0001)_{Mg}.$$

ED patterns of β'' phase overlap with that of the α'-Mg matrix so that reflections of the β'' phase are exactly in the middle between those of the α'-Mg matrix or exactly overlap with them (see in Fig. 1b the simulated ED pattern to Fig. 1a). Due to the equiaxial orientation no extra diffraction spots can be generated by dynamic effects (double diffraction). Also ED patterns from all equivalent orientation modes of the β'' phase overlap exactly each other. Diffraction spots from fine

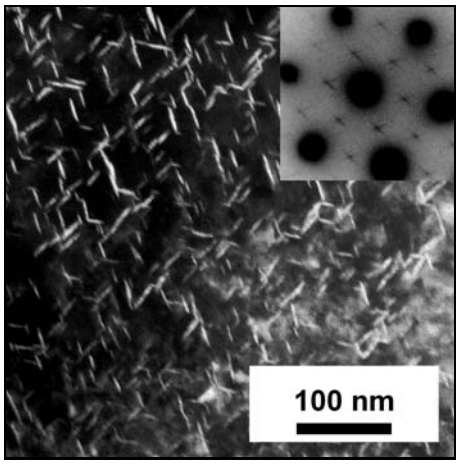

Fig. 2. Thin plates of $D0_{19}$ phase parallel to $\{11\bar{2}0\}_{Mg}$ planes. $[0001]_{Mg}$ pole, see ED patterns in inset, reflections of $D0_{19}$ as streaks in $\langle 11\bar{2}0\rangle_{Mg}$ directions.

thin plates are elongated in the direction perpendicular to the habit plane (Fig. 2). It makes possible to identify the habit plane also in the case, when the image is masked by some artefacts (e.g. oxides) due to the thin foil preparation. Lengths of the streaks can also yield an estimate of plate thickness.

2.2 β' transient phase (Cbco)

β' transient phase has Cbco structure mentioned above in the alloys containing R.E. from the Gd(Y) group (Table 2). It precipitates also in the alloys with combination of R.E. elements from different groups (e.g. WE54, WE43), see Table 2. Cbco phase precipitates in the following orientation relationship to the α'-Mg matrix in all alloys where it was detected:

$$[001]_{Cbco} \| [0001]_{Mg},$$
$$(100)_{Cbco} \| \{11\bar{2}0\}_{Mg}.$$

Originally it was reported to have $\{1\bar{1}00\}_{Mg}$ habit plane [1, 5]. Recent investigation on Mg-Gd and WE alloys has shown, that plate-like form of the Cbco phase has $\{11\bar{2}0\}_{Mg}$ habit plane but also $\{1\bar{1}00\}_{Mg}$ plane was reported (Table 2). In alloys with a combination of R.E. from different groups also globular form of the Cbco phase was found [11, 14–17]. Globular particles are the nucleation sites for another transient phase (isomorphous with transient β' fcc phase of Mg-Ce system), here it is usually reported as β_1.

All equivalent orientation modes of the Cbco phase precipitate simultaneously so the overlapping of all ED patterns that suit to the orientation relationship was observed – see in Fig. 3a $[0001]_{Mg}$ ED pattern from Mg15Gd alloy overlapped with

Table 2. Overview of the occurrence conditions and orientation of β' phase (Cbco)

Alloy composition [wt.%]	Treatment; temperature [°C] not plate-like shape	Habit plane of plates	Ref.
Mg-10Y	isothermal 200–300 both as β'' and β'	$\{1\bar{1}00\}_{Mg}$	[5]
Mg-5.08Y-2.96Nd-0.4Zr	isothermal 200–250	$\{1\bar{1}00\}_{Mg}$	[5]
Mg-6.85MM-1.82Nd-0.52Zr MM = 75 % Y + 25 % heavy R.E.	isothermal 200–250	$\{1\bar{1}00\}_{Mg}$	[5]
Mg-2.985Nd	isothermal 200–320 discs, monocl. structure	$\{1\bar{1}00\}_{Mg}$	[23]
Mg-14.55Gd	isochronal 280	$\{11\bar{2}0\}_{Mg}$	[10]
Mg-4Y-3.3R.E.-0.5Zr(WE43)	isothermal 150, 1896 h	$\{11\bar{2}0\}_{Mg}$	[14]
Mg-4Y-3.3R.E.-0.5Zr(WE43)	isothermal 250, 2–8 h	$\{11\bar{2}0\}_{Mg}$	[14]
Mg-4Y-3.3R.E.-0.5Zr(WE43)	isothermal 150, 1324 h; 250, 2–16 h; globular	–	[14]
Mg-4Y-2.25Nd-0.6Zr	isothermal 250, 2 h globular	–	[12]
Mg-9.5Gd-3Nd-0.4Zr Mg-9.3Dy-3.2Nd-0.4Zr Mg-10.8Gd-3Y-0.45Zr Mg-10.8Gd-6.6Y-0.36Zr	isothermal 225, 16–64 h Cbco coexists with $D0_{19}$	?	[24]
Mg-3Gd-8Y-0.8Zr Mg-6Gd-5Y-0.8Zr Mg-10Gd-3Y-0.7Zr	isothermal 225, 128 h isothermal 225, 32 h isothermal 225, 8 h Cbco coexists with $D0_{19}$	?	[7]
Mg-16.9Gd-0.51Zr Mg-12Gd-1.9Y-0.69Zr Mg-9.3Gd-4.1Y-0.7Zr	isothermal 250, $\sim$ 100 h Cbco coexists with $D0_{19}$	?	[25]
WE54	isothermal 250, 4 h, 48 h globular on β "	–	[11, 15, 16]
WE54	6 % cold work + annealing 250, 4 h, globular	–	[16]
WE54	isothermal 200, 72 h	?	[16]
WE43	isothermal 200, 300 h	plates	[27]
Mg-6Y	isothermal 150, 144 h	$\{1\bar{1}00\}_{Mg}$	[28]
Mg-8.3wt.%Y Mg-10.7wt.%Y	isothermal 230, 48–96 h 270, 24–48 h 277 crept + 270, 10 h	–	[29]

all orientations of $[001]_{Cbco}$ patterns. Simulated ED patterns with a single orientation of Cbco (Fig. 3b) rotated 60 and 120 degrees and overlapped (Fig. 3c) exactly match the experimental patterns. Similarly, $[44\bar{8}3]_{Mg}$ patterns from peak hardened

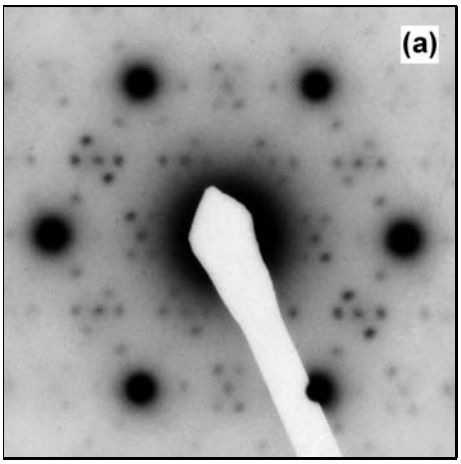

Fig. 3a. ED pattern of Mg15Gd alloy with all orientation modes of Cbco phase plates, $[0001]_{Mg}$ pole.

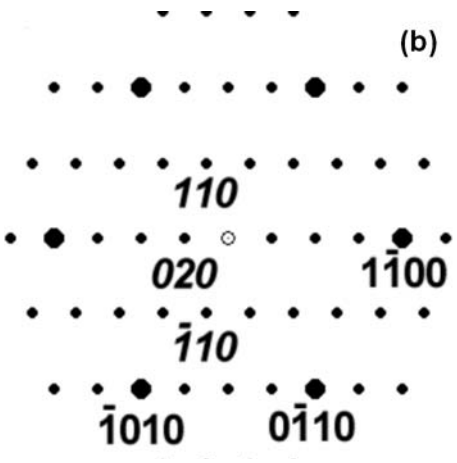

Fig. 3b. Simulated $[0001]_{Mg}$ pole pattern with single orientation mode of Cbco plates.

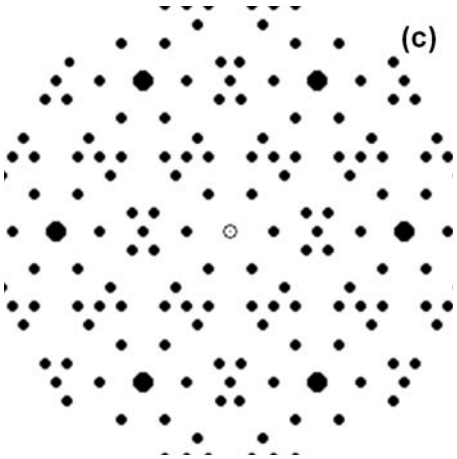

Fig. 3c. Simulated $[0001]_{Mg}$ pole pattern with all orientation modes of Cbco plates.

Mg15Gd alloy (Fig. 4a) can be unambiguously interpreted as the overlapping of matrix pattern with $[\bar{2}01]$ (Fig. 4b) and two $\langle 212 \rangle$ (Fig. 4c) patterns of Cbco phase (Fig. 4d).

In the recent paper on the precipitation in WE43 [14], the authors suggest a body centred orthorhombic structure for the β' phase instead of the C base centred one. Unambiguous determination of the correct Bravais lattice is difficult here as the missing reflections in some ED patterns of bco lattice can appear by

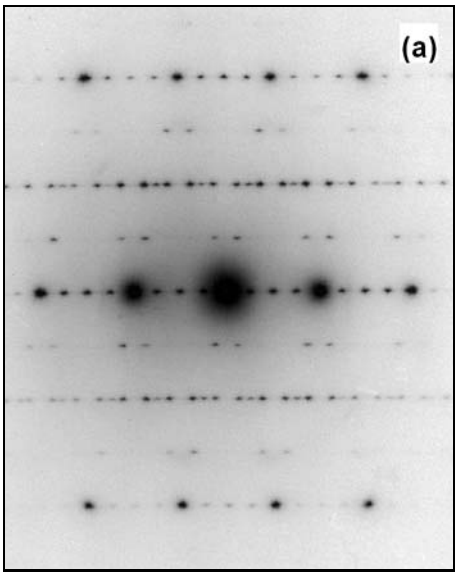

Fig. 4a. $[44\bar{8}3]_{Mg}$ pole ED pattern of the same alloy as in Fig. 3a.

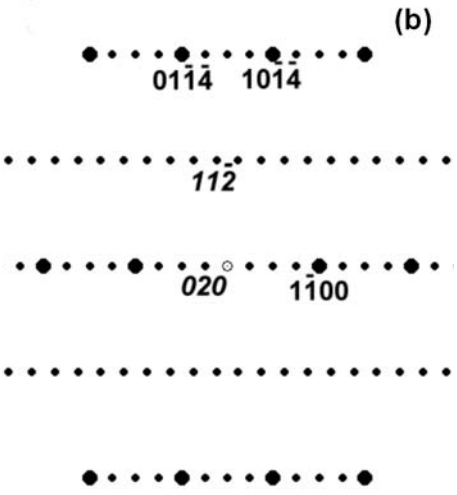

Fig. 4b. Simulated $[44\bar{8}3]_{Mg}$ pole ED pattern overlapped with $[201]_{Cbco}$ pattern.

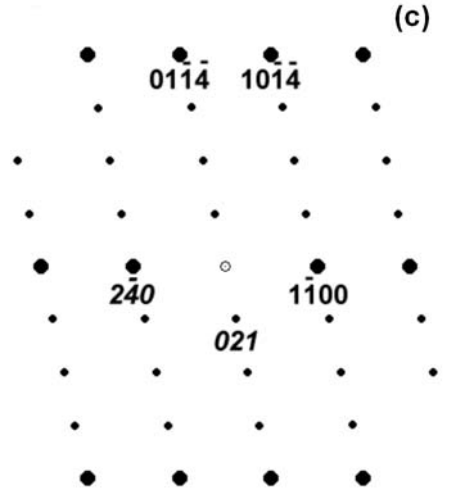

Fig. 4c. Simulated $[44\bar{8}3]_{Mg}$ pole ED pattern overlapped with $[\bar{2}\bar{1}2]_{Cbco}$ pattern.

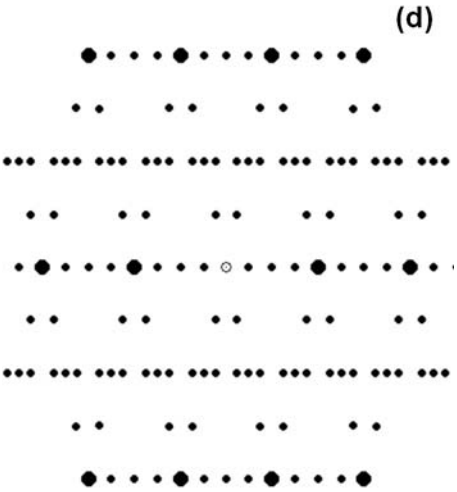

Fig. 4d. Simulated $[44\bar{8}3]_{Mg}$ pole ED pattern overlapped with Cbco patterns of all equivalent orientation modes.

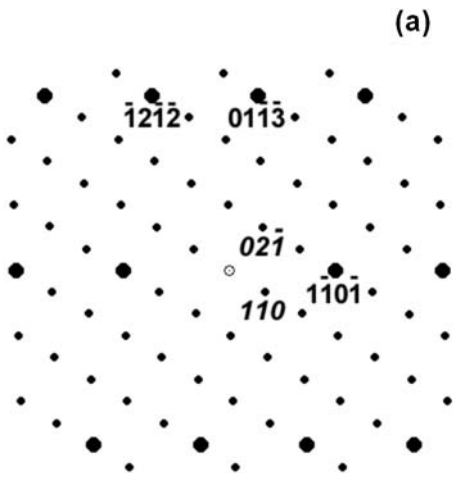

Fig. 5a. Simulated $[52\bar{7}3]_{\mathrm{Mg}}$ patterns with $[\bar{1}12]_{\mathrm{Cbco}}$ pattern.

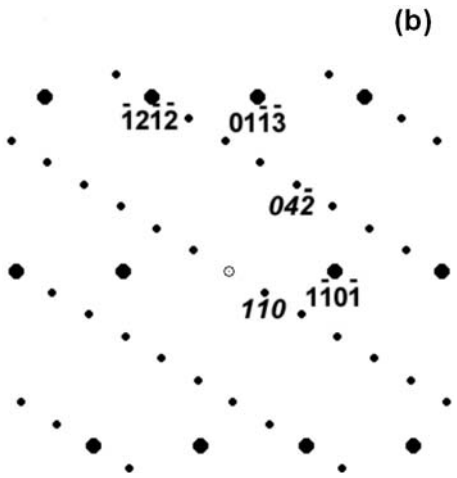

Fig. 5b. As in Fig. 5a with pattern of bco modification of β' phase.

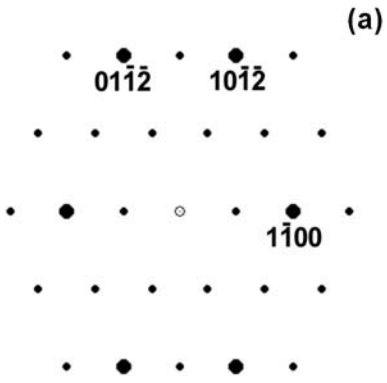

Fig. 6a. Simulated overlapping of $[22\bar{4}3]_{\mathrm{Mg}}$ pole pattern with $[11\bar{2}3]_{\mathrm{D0_{19}}}$ pole pattern.

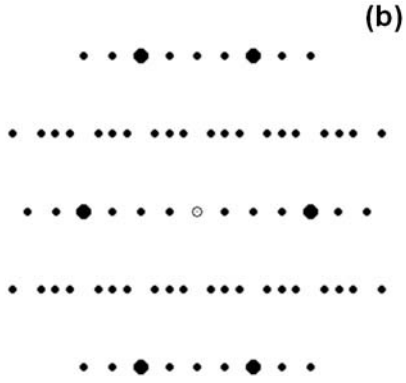

Fig. 6b. Simulated $[22\bar{4}3]_{\mathrm{Mg}}$ pole pattern with $<214>_{\mathrm{Cbco}}$ and $<101>_{\mathrm{Cbco}}$ pole patterns.

double diffraction and so the patterns would remind those of Cbco ED patterns – cf. Figs. 5a,b. Fourier transform of the HRTEM image of single particles can help, but thorough check of the image interpretation is essential [14].

Some authors (Tables 1 and 2) reported coexistence of $D0_{19}$ and Cbco plates. Again, to decide if both phases are really present is difficult on the basis of selected

area ED (SAED) only, as reflections of $D0_{19}$ and Cbco overlap, cf. overlapping of $[22\bar{4}3]_{\mathrm{Mg}}$ with $[11\bar{2}3]_{D0_{19}}$ patterns in Fig. 6a and with $\langle 214\rangle_{\mathrm{Cbco}}$ and $\langle 101\rangle_{\mathrm{Cbco}}$ patterns in Fig. 6b. HRTEM and Fourier transforms are needed here, too.

On the other hand, to decide if the Cbco phase already coexists with $D0_{19}$, such ED patterns of matrix should be analysed which contain Cbco reflections not overlapping with $D0_{19}$ ones – e.g. $[44\bar{8}3]_{\mathrm{Mg}}$ (Figs. 4b-d) instead of $[22\bar{4}3]$Mg (Fig. 6). So it seems that the Cbco phase already coexists with $D0_{19}$ after isothermal treatment of the Mg-4Y-2.25Nd-0.6Zr alloy at 150 ℃ for 5000 h [17] contrary to the authors interpretation and to the Mg-7Gd-2.25Nd-0.6Zr alloy after the same treatment. In the latter alloy the streaks in the $[0001]_{\mathrm{Mg}}$ pole ED pattern (Fig. 1 there) in $\langle 11\bar{2}0\rangle_{\mathrm{Mg}}$ directions really belong to the $D0_{19}$ reflections, in the former alloy the streaks in $\langle 10\bar{1}0\rangle_{\mathrm{Mg}}$ directions are in fact reflections from Cbco phase. Of course, another pole ED patterns should be also analysed, e.g. $[44\bar{8}3]_{\mathrm{Mg}}$. The same line of reasoning can be used for the diffraction patterns of WE43 alloy annealed 864 h at 150 ℃ [14]. In both $[0001]_{\mathrm{Mg}}$ and $[\bar{2}110]_{\mathrm{Mg}}$ pole patterns (Fig. 2 there) the streaks are in fact the reflections from Cbco phase.

2.3 β_1 (β') transient phase ($D0_3$, fcc)

The transient β' phase of the Mg-Ce system precipitates also in the form of prismatic plates parallel to the $\{1\bar{1}00\}_{\mathrm{Mg}}$ planes [18]. It has following orientation relationship to the α'-Mg matrix:

Table 3. Overview of the occurrence conditions and orientation of β_1 phase (fcc)

Alloy composition [wt.%]	Treatment; temperature [℃] not plate-like shape	Habit plane of plates	Ref.
Mg-3Nd	isothermal 200–300	–	[5]
Mg-1.3MM MM = 50 Ce, 25 La, 20 Nd, 3 Pr	200, 3 h β' coexists with β	$\{1\bar{1}00\}_{\mathrm{Mg}}$	[18]
WE54	isothermal 250, 4 h	$\{1\bar{1}00\}_{\mathrm{Mg}}$	[16]
WE54	cold rolled 6 % and 12 % + annealing 250, 4 h	$\{1\bar{1}00\}_{\mathrm{Mg}}$	[16]
WE54	isothermal 250, 48 h	$\{1\bar{1}00\}_{\mathrm{Mg}}$	[11, 15]
Mg-4Y-2.25Nd-0.6Zr Mg-7Dy-2.25Nd-0.6Zr Mg-7Gd-2.25Nd-0.6Zr	isothermal 250, 8 h	$\{1\bar{1}00\}_{\mathrm{Mg}}$	[12]
WE43	isothermal 250, 16 h nucleate on globular Cbco	$\{1\bar{1}00\}_{\mathrm{Mg}}$	[14]

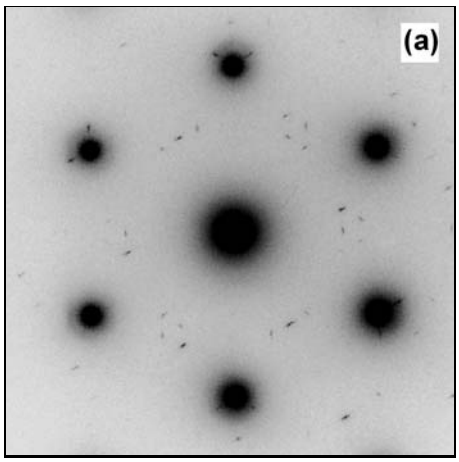

Fig. 7a. $[0001]_{Mg}$ ED pole pattern of Mg--4Tb-2Nd alloy with all equivalent patterns of β_1 plates parallel to $\{1\bar{1}00\}_{Mg}$ planes.

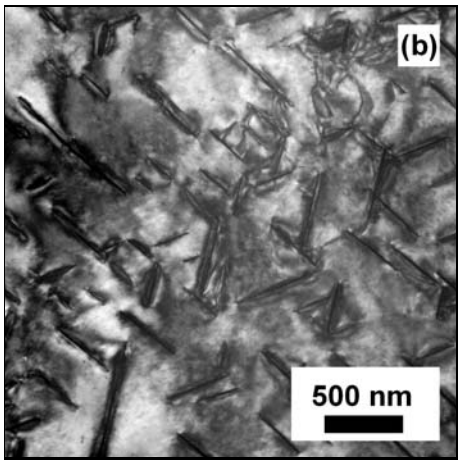

Fig. 7b. Bright field image of the alloy in the orientation shown in Fig. 7a.

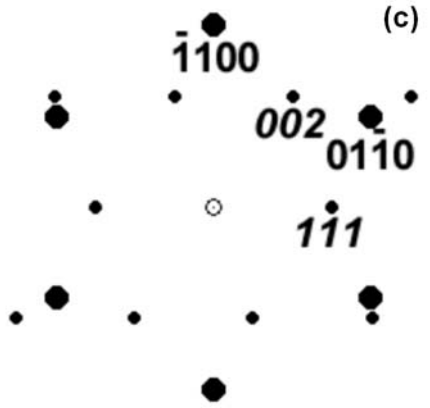

Fig. 7c. Simulated $[0001]_{Mg}$ pole pattern overlapped with one of $<110>_{\beta 1}$ pole pattern.

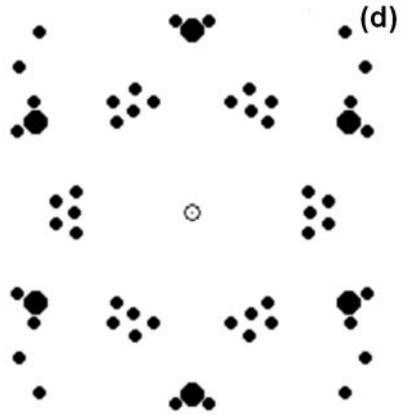

Fig. 7d. Simulated $[0001]_{Mg}$ pole pattern overlapped with patterns of all equivalent orientation modes of β_1 phase.

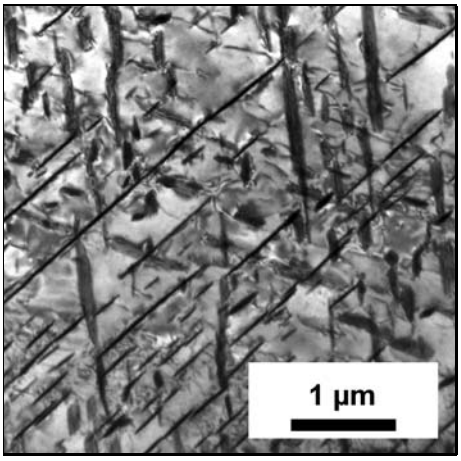

Fig. 8. Coarse prismatic plates of β phase parallel to $\{1\bar{1}00\}_{Mg}$ planes. $[0001]_{Mg}$ pole, overaged Mg-6Y-3Nd-0.5 Zr alloy.

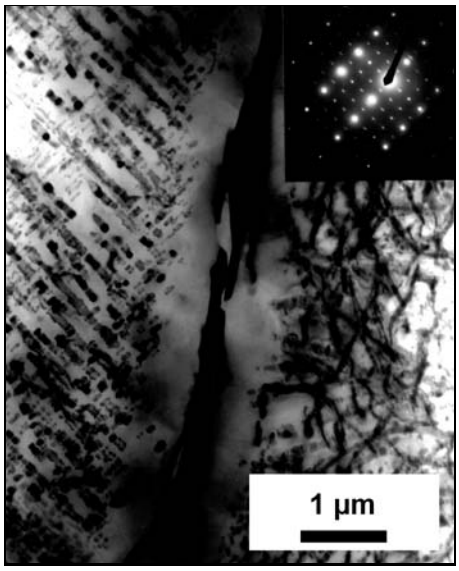

Fig. 9. Thread-like modification of $Mg_{12}Nd$ phase in isochronally annealed QE22 alloy [13].

$$(0001)_{Mg} \| \{1\bar{1}0\}_{D0_3},$$
$$\langle 11\bar{2}0\rangle_{Mg} \| \langle 111\rangle_{D0_3}.$$

The same structure $D0_3$, habit plane and orientation to the matrix was found for transient β_1 phase in Mg alloys with the combination of R.E. from different groups (Table 3).

In SAED patterns of Mg alloys with β_1 plates all ED patterns of the β_1 phase orientation modifications which suit the orientation relationship do overlap – see Fig. 7a the [0001] pole patterns from Mg-4Tb-2Nd alloy with β_1 phase plates (Fig. 7b) and simulated patterns in Figs. 7c,d. It is very difficult to detect the early stages of β_1 phase precipitation as the stronger reflections from Cbco and/or $D0_{19}$ phases mask weak and diffuse reflections from the β_1 phase. HRTEM and Fourier transforms can be helpful tools here again.

2.4 β equilibrium phases (fcc, bcc, bct)

Equilibrium β phases in Mg-R.E. base alloys with fcc (isomorphous with Mg_5Gd) and bcc (isomorphous with $Mg_{24}Y_5$) structure precipitate also in the form of coarser plates with $\{1\bar{1}00\}_{Mg}$ habit plane (Fig. 8). Both phases have the same

orientation relationship to the α'-Mg matrix as the β_1 phase has. The composition and parameters are dependent on the alloy composition and heat treatment applied.

It is not possible to simply apply decomposition sequences of binary alloys to Mg alloys with combination of R.E. elements. Not necessarily should the structure of an equilibrium phase agree with that of the binary Mg alloy with the majority element, as some authors argue [19]. So the equilibrium β phase in all WE alloys has the fcc structure (Mg_5Gd) instead of a bcc ($Mg_{24}Y_5$) – e.g. [5, 6, 11, 17] etc.

The equilibrium phase in Mg alloys with R.E. of Ce group does not precipitate in the form of prismatic plates. It has body centred tetragonal structure either tI26 ($Mg_{12}Ce$, $a = 1.033$ nm, $c = 0.596$ nm) or tI92 ($Mg_{41}Nd_5$, $a = 1.476$ nm, $c = 1.039$ nm) [5, 30, 31]. Peculiar metastable morphology of the β phase (thread-like $Mg_{12}Nd$) was observed in isochronally annealed QE22 alloy (Mg-Ag-Nd-Zr) [13] (Fig. 9). Both metastable modification of $Mg_{12}Nd$ and stable $Mg_{12}Ce$ have the following orientation relationship to the α'-Mg matrix:

$$(0001)_{\mathrm{Mg}} \| (100)_{\mathrm{bct}},$$
$$\langle \bar{1}100 \rangle_{\mathrm{Mg}} \| \langle 0\bar{1}1 \rangle_{\mathrm{bct}}.$$

Transient phase with the same structure and orientation was observed in ribbon-like morphology in as cast complex Mg-Ce-Sc-Mn alloy [20, 21].

2.5 Transient phases of R.E. with addition elements in complex Mg-R.E. base alloys

Additive elements such as Zn, Mn etc. are used to improve mechanical properties of Mg-R.E. base alloys, e.g. [20, 22]. A common feature observed in alloys with these additions is a precipitation of thin plates parallel to the basal plane of the α'-Mg matrix. The plates contain corresponding addition element and R.E. (e.g. Y and/or Gd respectively). The ordered hexagonal structure was suggested for these defects interpreted as GP zones [22]. They have following orientation relationship to the α'-Mg matrix [3, 20]:

$$\langle 10\bar{1}0 \rangle_{\mathrm{hp}} \| \langle 11\bar{2}0 \rangle_{\mathrm{Mg}},$$
$$(0001)_{\mathrm{hp}} \| (0001)_{\mathrm{Mg}}.$$

The main feature of diffraction patterns are long streaks of intensity in $[0001]_{\mathrm{Mg}}$ direction. Lattice parameter $a \cong 2 \cdot d\{1\bar{1}00\}_{\mathrm{Mg}} = 0.556$ nm, $c = c_{\mathrm{Mg}}$. Not all reflections in different poles of the α'-Mg matrix ED patterns can be interpreted on the base of this lattice and parameters. In fact, they can be unambiguously interpreted as the intersections of the streaks mentioned above with the Ewald sphere.

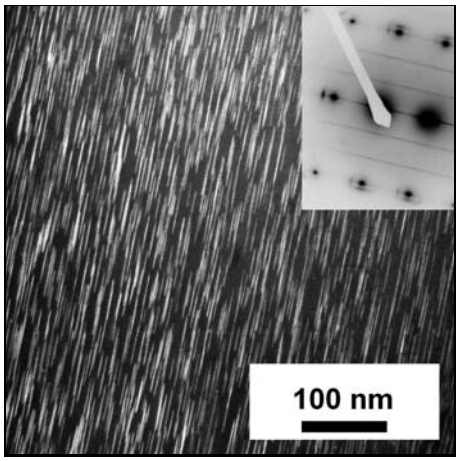

Fig. 10. Very dense arrangement of thin plates parallel to the basal plane in Mg-4Y--2Nd-1Zn-1Mn alloy. $[1\bar{1}00]_{Mg}$ pole pattern in inset, notice intensity streaks perpendicular to basal plane.

Figure 10 shows very dense arrangement of thin basal plates in MgYNdZnMn alloy. The spots in ED patterns corresponding to the intersection of streaks with Ewald sphere were observed to change their position continuously during tilting this specimen from one to another pole.

3. Conclusion

The analysis of phase structure, form and orientation of precipitates, etc. is possible by means of a conventional transmission electron microscopy and electron diffraction if care is taken of all possible peculiarities and problems. They are connected mainly with a dynamic character of electron diffraction (double diffraction) and with morphology and form of phases (dimension effect in ED, simultaneous precipitation of all equivalent modifications, an overlapping of the ranges of transient phases occurrence etc.). High resolution transmission electron microscopy, microdiffraction and Fourier transform of HRTEM images of single particles are more and more gaining on importance in the phase analysis of Mg alloys.

Acknowledgements

The support by the German Research Foundation (DFG), by the Czech Scientific Foundation (GACR project 106/03/0903) and by the Ministry of Education of Czech Republic within the framework of the research programme MSM 113200002 are gratefully acknowledged.

The authors would like to congratulate Prof. Dr. Petr Kratochvíl, DrSc., to his 70^{th} birthday.

REFERENCES

[1] POLMEAR, I. J.: Mater. Sci. Technol., *10*, 1994, p. 1.
[2] MORDIKE, B. L.: J. Jilm, *51*, 2001, p. 1.
[3] SMOLA, B.—STULÍKOVÁ, I.—VON BUCH, F.—MORDIKE, B. L.: Mater. Sci. Eng. A, *324*, 2002, p. 113.
[4] STULÍKOVÁ, I.—SMOLA, B.—VON BUCH, F.—MORDIKE, B. L.: Mat.-wiss. u. Werkstofftech., *34*, 2003, p. 102.
[5] LORIMER, G. W.: In: Proc. London Conf. Magnesium Technology. Ed.: Baker, H. London, Inst. of Metals 1986, p. 47.

[6] VOSTRÝ, P.—STULÍKOVÁ, I.—SMOLA, B.—CIESLAR, M.—MORDIKE, B. L.: Z. Metallkd., *79*, 1988, p. 340.
[7] ANYANWU, I. A.—KITAGUCHI, Y.—HARIMA, Y.—KAMADO, S.—KOJIMA, Y.—TANIKE, S.—SEKI, I.: In: Magnesium 97. Eds.: Aghion, E., Eliezer, D. Beer-Sheva, MRI, Ltd. 1998, p. 127.
[8] NIE, J. F.: Scripta Mater., *48*, 2003, p. 1009.
[9] STULÍKOVÁ, I.—SMOLA, B.—CIESLAR, M.—HÁJEK, M.—PELCOVÁ, J.—MELIKHOVA, O.—FALTUS, J.: Kovove Mater., *40*, 2002, p. 321.
[11] NIE, J. F.—MUDDLE, B. C.: Acta Mater., *48*, 2000, p. 1691.
[12] APPS, P. J.—KARIMZADEH, H.—KING, J. F.—LORIMER, G. W.: Scripta Mater., *48*, 2003, p. 1023.
[13] KIEHN, K.—SMOLA, B.—VOSTRÝ, P.—STULÍKOVÁ, I.—KAINER, K. U.: Phys. stat. sol. (a), *164*, 1997, p. 709.
[14] ANTION, C.—DONNADIEU, P.—PERRARD, F.—DESCHAMPS, A.—TASSIN, C.—PISCH, A.: Acta Mater., *51*, 2003, p. 5335.
[15] NIE, J. F.—MUDDLE, B. C.: Scripta Mater., *40*, 1999, p. 1089.
[16] HILDITCH, T.—NIE, J. F.—MUDDLE, B. C.: In: Magnesium Alloys and their Application. Eds.: Mordike, B. L., Kainer, K. U. Frankfurt, Werkstoff-Informationsgesellschaft mbH 1998, p. 339.
[17] APPS, P. J.—KARIMZADEH, H.—KING, J. F.—LORIMER, G. W.: Scripta Mater., *48,* 2003, p. 1023.
[18] WEI, L.Y.—DUNLOP, G. L.—WESTENGEN, H.: J. Mater. Sci., *31*, 1996, p. 387.
[19] ROKHLIN, L. L.—DOBATKINA, T. V.—TARYTINA, I. E.—TIMOFEEV, V. N.—BALAKHCHI, E. E.: J. Alloys Comp., *367*, 2004, p. 17.
[20] SMOLA, B.—STULÍKOVÁ, I.—PELCOVÁ, J.—VON BUCH, F.—MORDIKE, B. L.: Z. Metallkd., *94*, 2003, p. 553.
[21] NEUBERT, V.—STULÍKOVÁ, I.—SMOLA, B.—BAKKAR, A.—MORDIKE, B. L.: Kovove Mater., *42*, 2004, p. 31.
[22] PING, D. H.—HONO, K.—NIE, J. F.: Scripta Mater., *48*, 2003, p. 1017.
[23] PIKE, T. J.—NOBLE, B.: J. of Less-Common Metals, *30*, 1973, p. 63.
[24] KAMADO, S.—KOJIMA, Y.: In: Proceedings of the 3rd International Magnesium Conference. Ed.: Lorimer, G. W. Cambridge, Inst. of Materials 1997, p. 327.
[25] KAMADO, S.—KOJIMA, Y.—TANIIKE, S.—SEKI, I.—HAMA, S.: In: Magnesium Alloys and their Application. Eds.: Mordike, B. L., Kainer, K. U. Frankfurt, Werkstoff-Informationsgesellschaft mbH 1998, p. 169.
[26] HISA, M.—BARRY, J. C.—DUNLOP, G. L: In: Proceedings of the 3rd International Magnesium Conference. Ed.: Lorimer, G. W. Cambridge, Inst. of Materials 1997, p. 369.
[27] WANG, J. G.—HSIUNG, L. M.—NIEH, T. G.—MABUCHI, M.: Mat. Sci. Eng. A, *315*, 2001, p. 81.
[28] SOCJUSZ-PODOSEK, M.—LITYNSKA, L.: Mat. Chem. Phys., *80*, 2003, p. 472.
[29] SUZUKI, M.—RIMURA, T.—MARUYAMA, K.—OIKAWA, H.: In: Creep and Fracture of Engineering Materials and Structures. Ed.: Parker, J. D. London, Inst. of Materials 2001, p. 147.
[30] MASSALSKI, T. B.: Binary Alloys Phase Diagrams. 2nd ed. Materials Park, OH, American Soc. for Materials 1990.
[31] VILLARS, P.—CALVERT, L. D.: Pearson's Handbook of Crystallographic Data for Intermetallic Phases. Materials Park, OH, ASM International 1991.

Received: 26.4.2004